An Electron Localization Function Study of the Lone Pair

D. B. Chesnut†

P. M. Gross Chemical Laboratory, Duke University, Durham, North Carolina 27708

Received: August 15, 2000; In Final Form: October 16, 2000

Electron localization function (ELF) theory is used to characterize lone pairs in a variety of situations. Using the lone pair basin attractor locations, lone pair distances from their parent nucleus may be defined as well as the angular disposition of the lone pair with regard to its neighboring atoms and bond basin centers. Studies of the first and second row hydrides show, with some exceptions, that lone pairs are basically tetrahedrally disposed with distances dependent essentially only on the atomic number (Z) of the heavy atom, decreasing with increasing Z. The examination of three-to-six membered heterorings involving nitrogen and phosphorus show that only in the most constrained systems are large effects noticeable. Two relatively weak hydrogen bonding systems ($HOH\cdots OH_2$ and $FH\cdots NH_3$) show that only a very small transfer of charge occurs upon dimer formation and involves mainly the proton donor and the acceptor lone pair; in the water dimer it is shown that *both* the acceptor lone pair and the donor proton lie off the line connecting the two oxygen atoms. Finally, examination of several model gauche and anti isomers containing ether oxygens shows that in the more stable gauche form a small but noticeable transfer of charge occurs from the interacting lone pair to the adjoining carbon bonding basin, a result consistent with the generally accepted double-bond/no-bond σ^* orbital interaction model of the anomeric effect in organic stereochemistry.

Introduction

The lone pair has played a key role in chemistry and is widely invoked in a variety of situations. Models like the valence shell electron repulsion theory[1,2] (VSEPR), recently quantified,[3] employ orbital models with lone pairs to predict their geometrical location and size effects in determining molecular structure. Molecular orbitals occupied by nonbonding electrons are important in the analysis of ab initio calculations. Orbitals, however, are not observables and often are not unique. The total electron density *is* an appropriate observable but the difficulty in quantifying the lone pair in this way arises from the fact that a molecule's electron density is typically relatively featureless on a detailed scale.

Bader[4] has shown in his atoms in molecule (AIM) approach that the second derivative of the total electron density can be used to reveal the location of bonding electron pairs as well as those that are nonbonding, the lone pairs. The electron localization function (ELF) of Becke and Edgecombe[5] is a somewhat more revealing approach; based on the powerful Pauli exclusion principle, its topological basins greatly resemble simple chemical pictures of where electrons, bonding and nonbonding, ought to be. It is the approach we take here to characterize molecular lone pairs in several chemically important situations. We look at the locations and characteristics of lone pairs in the first and second row hydrides, what the effect of ring strain is, how the lone pair properties are modified when hydrogen bonding occurs, and whether ELF is able to verify or disprove the currently accepted model of the anomeric effect in organic stereochemistry. Our treatment is not exhaustive but is sufficiently broad to give a good feel for the ELF characterization of these important chemical species.

† Phone: 919-660-1537. Fax: 919-660-1605. E-mail: dbc@chem.duke.edu.

The Electron Localization Function

ELF is a robust descriptor of chemical bonding based on topological analysis of local quantum mechanical functions related to the Pauli exclusion principle. It was first introduced by Becke and Edgecombe[5] and has been developed and applied extensively by Savin and Silvi and their collaborators.[6−13] The local maxima of the function define localization attractors corresponding to core, bonding (located between the core attractors of different atoms) and nonbonding electron pairs and their spatial arrangement. It is of special interest to chemists in that the resulting isosurfaces of ELF density tend to conform to the classical Lewis picture of bonding.

Becke and Edgecombe[5] pointed out that the conditional pair probability for same spin electrons has the form

$$P^{\sigma\sigma}_{\mathrm{cond}}(\bar{r},s) = \frac{1}{3}\left[\sum_{j}^{\sigma}\left|\nabla\varphi_j\right|^2 - \frac{1}{4}\frac{|\nabla\rho_\sigma|^2}{\rho_\sigma}\right]s^2 + \ldots \qquad (1)$$

for an electron at point $\bar{r}$ and another a distance s away (averaged over a spherical shell of radius s). The coefficient of the quadratic term is the local Pauli kinetic energy density, the excess kinetic energy electrons have (due to the Pauli exclusion principle) compared to a bosonic system of the same density.[8] When it is small the Fermi hole at $\bar{r}$ is large and one would expect to find pairs of electrons of *opposite* spin in the region; when it is large, the converse is true.

For a closed shell single determinantal wave function built from Hartree−Fock or Kohn−Sham orbitals, φ_j, the ELF function of position $\bar{r}$ is *defined* as

$$\eta = \frac{1}{1+\left(\frac{D}{D_h}\right)^2} \qquad (2)$$

10.1021/jp002957u CCC: $19.00
Published on Web 11/17/2000

where

$$D = \frac{1}{2}\sum_{j=1}^{N}|\nabla\varphi_j|^2 - \frac{1}{8}\frac{|\nabla\rho|^2}{\rho}$$

$$D_h = \frac{3}{10}(3\pi^2)^{2/3}\rho^{5/3}$$

$$\rho = \sum_{j=1}^{N}|\varphi_j|^2 \qquad (3)$$

and where the scaling factor was chosen to be the homogeneous electron gas kinetic energy density of a system of the same density. The ELF function can be viewed as a local measure of the Pauli repulsion between electrons due to the exclusion principle and allows one to define regions of space that are associated with different electron pairs in a molecule or solid. The position where ELF attains a maximum value (the attractor) can be used as an electron pair's signature.[11]

Using the vector field of the gradient of the electron localization function, the topology of the ELF function can be used to define basins within which one or more electron pairs are to be found.[7−9,12] These subsystems are defined in terms of zero flux surfaces; the gradient paths end at what are called *attractors* within each subsystem. The region of three-dimensional space traversed by all gradient paths that terminate at a given attractor defines the *basin* of the attractor. ELF basins are labeled as either core or valence basins. Core basins contain a nucleus while valence basins do not; hydrogen basins are taken as exceptions since, although they contain a proton, they represent a shared pair interaction. A valence basin is characterized by its number of connections to core basins, referred to as its synaptic order. Basins are connected if they are bounded by part of a common surface. A simple covalent bond basin would be connected to two core basins and be of synaptic order two; a lone pair basin would be monosynaptic. More complex bonding basins can be polysynaptic.

The population of a basin Ω_i, N_i, is given by integrating the total electron density, $\rho(\bar{r})$, over the basin volume. These populations are particularly important in that they tend

$$N_i = \int_\Omega \rho(\bar{r})\, d\bar{r} \qquad (4)$$

to reflect delocalization effects and, in the case of bond basins, the bond order.

ELF has been applied to some rather complex problems in chemistry including elementary chemical reactions,[14] the study of excited states,[15] the determination of protonation sites in bases,[16] orienting effects in electrophilic aromatic substitutions reactions,[17] the direct space representation of the metallic bond,[18] and the characterization of hydrogen bonds of varying degree of strength.[19] Besides looking at ELF isosurfaces and populations many of these new applications deal with such subtleties as the ELF bifurcation points and the value of ELF at inter-attractor critical points (the value of ELF at certain saddle points).

Theoretical Details

The ELF calculations were carried out employing the TopMod Package of Noury and co-workers[20] in the B3LYP approach[21,22] both for geometry optimization and for calculating the electron localization function. The B3LYP/6-31+G(d,p) level was employed for the simple hydrides and the B3LYP/6-31+G(d) level for the other compounds; when comparisons had to be made between the large molecules and the hydrides, the pertinent hydrides were recalculated at the B3LYP/6-31+G(d) level. Step sizes of 0.1 au and box sizes that extended 5.0 au from the outermost atomic coordinates in each direction were typically used. The TopMod package sacrifices some accuracy for efficiency and, according to the authors,[20] is thought to be accurate to a few percent, sufficient for comparative studies. For some of the more accurate energy determinations the B3LYP/6-311++G(3df,2p)//B3LYP/6-31+G(d) approach was used. All the optimization and energy calculations were carried out with Gaussian 98.[23]

TABLE 1: XH Bond Lengths and Distances of Lone Pairs to Their Corresponding Core Basin (r_{XH}, r_{lp}, Å), Angles Involving the Lone Pairs and Hydrogen Atoms (∠lp−l*p*, ∠lp−H, ∠H−H, Degrees), and Lone Pair Basis Populations (N_{lp}, Electrons)[a]

	r_{lp}	r_{XH}	∠lp−lp	∠lp−H	∠H−H	N_{lp}
CH_3^-	1.474	1.104		108.9	110.1	1.63
CH_2^{2-}		1.127			107.1	3.74[b]
NH_3	0.776	1.016		110.8	108.2	2.02
NH_2^-	0.694	1.035	93.1	115.5	102.8	2.01 (2)
H_2O	0.584	0.969	107.6	111.1	105.4	2.27 (2)
H_3O^+	0.583	0.982		104.9	113.8	2.06
H_3F^+	0.497	0.972	115.7	106.8	114.6	2.42 (2)
H_3F^{2+}	0.481	1.079	180.0	90.0	120.0	1.86 (2)
SiH_3^-	1.296	1.548		121.6	95.2	1.96
SiH_2^{2-}	1.225[c]	1.568	68.6[c]	124.4[c]	93.8	3.74[a]
PH_3	1.115	1.424		122.5	93.6	2.14
PH_2^-	1.119	1.442	118.4	110.8	92.1	1.99 (2)
H_2S	0.985	1.348	124.5	108.7	92.7	2.13 (2)
H_3S^+	0.971	1.360		121.3	95.1	2.24
H_2Cl^+	0.872	1.315	122.5	108.8	95.7	2.21 (2)
H_2Cl^{+3}	0.865	1.383		118.2	99.3	2.35

[a] A "2" in parentheses indicates two equivalent basins at the indicated value. The XH distances and H−H angles were taken from the B3LYP/6-31+G(d) nuclear geometries. [b] Total lone pair population. [c] Data from the two major lone pair basins.

The ELF basins together span the entire molecular space and individually have finite extents that vary according to the type of electrons they contain. In contrast to a core basin, lone pair or bonding basins do not contain a nuclear center (with the exception of hydrogen basins which are counted as bonding basins). The lone pair basin attractor (basin ELF maximum) is taken here as the geometrical location of the lone pair for purposes of determining lone pair distances to their parent nuclei and in determining lone-pair-nuclear angles. An ELF center of gravity might be another choice, but is one currently not available in the TopMod code. Using the lone pair basin attractor to define the mean position of the electrons involved seems eminently reasonable.

The First and Second Row Hydrides

With the exception of CH_2^{2-}, SiH_2^{2-}, and H_3F^{2+} (discussed below), all of the lone pair attractors assume the expected essentially tetrahedral positions in the hydrides; the distance and angular data are contained in Table 1. The lone pair distances, r_{lp}, measured from the heavy atom core attractors decline monotonically with increasing Z (atomic number) in a manner similar to the corresponding XH bond lengths. This is readily understood in terms of the nuclear charge pulling both bonding and lone pair electrons closer to the nucleus. CH_3^- has a large lone pair distance relative to the other first row hydrides; the reason for this is unclear. (One of the reviewers suggests that the ELF function may be very flat in this case, making the location of its attractor very sensitive. The sensitivity to basis is reflected in the fact that the lone pair distance is 1.29 Å in

TABLE 2: Effective Radii (Å) Per Basin Electron Calculated from $V_i/N_i = (4/3)\pi R_i^3$ for the Lone Pair (R_i^{lp}) and Hydrogen (R_i^H) Basins of the First and Second Row Hydrides

	R_i^{lp}	R_i^H		R_i^{lp}	R_i^H
CH_4		1.19	SiH_4		1.35
CH_3^-	1.65	1.20	SiH_3^-	1.72	1.40
CH_2^{2-}	2.05[a]	1.23	SiH_2^{2-}	2.20[a]	1.39
NH_3	1.19	1.09	PH_3	1.42	1.27
NH_2^-	1.41	1.16	PH_2^-	1.58	1.29
H_2O	1.04	1.02	H_2S	1.30	1.20
H_3O^+	0.96	0.96	H_3S^+	1.22	1.16
HF	0.91	1.04	HCl	1.19	1.14
H_2F^+	0.83	0.96	H_2Cl^+	1.12	1.10
H_3F^{2+}	0.77	0.95	H_3Cl^{2+}	1.09	1.08

[a] From the summed volumes and electron numbers of the total lone pair space.

the B3LYP/6-31G(d)//B3LYP/6-31+G(d,p) approach and 1.41 Å at the B3LYP/6-311++G(3df,2p)//B3LYP/6-31+G(d,p) level.) The atomic number of the heavy atom nucleus essentially determines r_{lp}, although NH_3 and NH_2^- do differ noticeably; the corresponding second row pair, NH_3 and PH_2^-, have virtually identical lone pair distances.

The VSEPR model[1−3] operates on the hypothesis that lone pairs are "larger" (more repulsive) than bond pairs and should, therefore, make larger angles with bond pairs and each other. The angle data in Table 1 shows this to be the case for the second row hydrides (without the exceptional case of SiH_2^{2-}; vide infra) but there are exceptions for the first row hydrides. The second row data likely reflect the fact that the HH angles are uniformly close to 95 degrees so that lone pairs in tetrahedral dispositions will of necessity make larger angles. That the first row data does not reflect the VSEPR predictions is likely another example of the fact that we do not yet fully understand the nuances of the ELF and AIM topographies. In both approaches the attractors are those points where the locater functions (η in ELF and the Laplacian of the electron density in AIM) are locally maximum and do not necessarily characterize electron pair repulsions per se.

A measure of the "size" of the lone pair and proton bonding basins is given in the TopMod output as the volume of the basin determined by integrating dV over the basin with a lower limit cutoff of $\eta = 0.02$. For convenience we define an effective basin radius, R_i, for the ith basin by

$$\frac{V_i}{N_i} = \frac{4}{3}\pi R_i^3 \qquad (5)$$

where V_i is the above-defined basin volume and N_i is the basin population in numbers of electrons. R_i, then, is the radius of the volume a single electron occupies in the basin in question; these data are given in Table 2. Again the R_i decrease monotonically with increasing Z and, while being larger than the corresponding hydrogen R_i in the left-hand portion of the periodic row, the two become comparable at the right-hand side of the periodic rows. In contrast to the case for the lone pair core distances, the R_i values now depend not only upon Z but also upon the net charge of the molecule. Increasing the negative charge on the molecule causes a noticeable increase in R_i while increasing the positive charge causes a decrease in R_i. As we might expect, the presence of negative charge causes the lone pair domains to become more diffuse while a positive overall charge results in more compact domains.

The exceptional cases mentioned above of CH_2^{2-}, SiH_2^{2-}, and H_3F^{2+} illustrate some of the complexities associated with

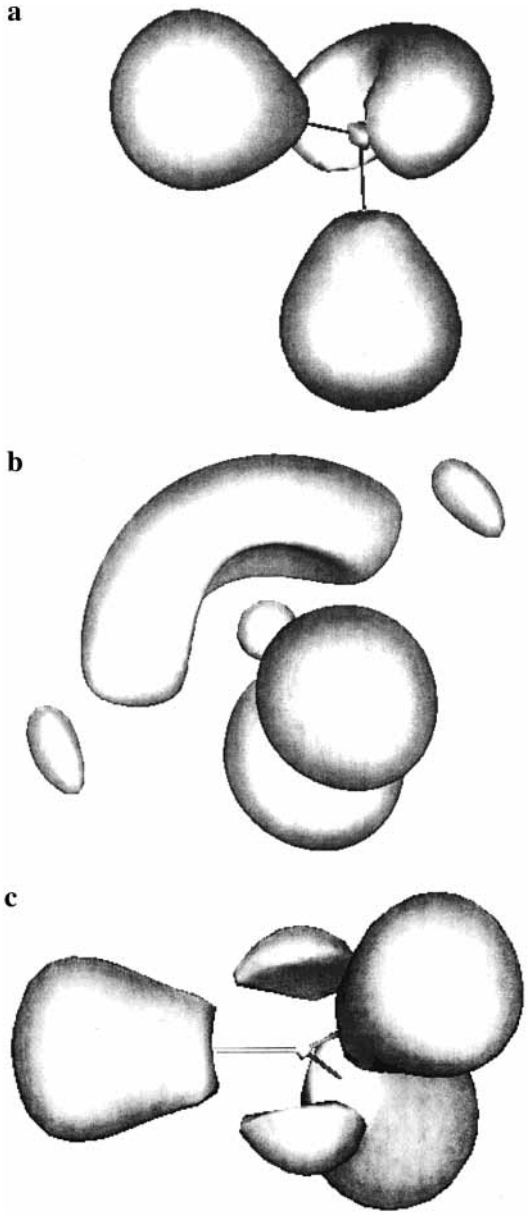

Figure 1. B3LYP/6-31+G(d,p)//B3LYP/6-31+G(d,p) ELF isosurfaces for (a) H_2O at $\eta = 0.85$, (b) SiH_2^{2-} at $\eta = 0.825$, and (c) H_3F^{2+} at $\eta = 0.864$.

ELF and the disposition of the ELF isosurfaces. Representative isosurfaces for H_2O, SiH_2^{2-}, and H_3F^{2+} are shown in Figure 1, with H_2O presented as an example of what is considered 'normal' behavior; that is, in the case of water the lone pairs are contained in two, essentially tetrahedrally oriented basins at right angles to the HOH plane. It is worthwhile mentioning that for most of the region of η the two water lone pairs are not separated and only do so, leading almost immediately to the two lone pair attractors very near the maximum η value for which the basins are extant. So while we take the lone pair basin attractors as measures of the mean location of these entities, for most of the time both lone pairs share common space.

The case of H_3F^{2+} is easily disposed of. This molecule is found to be planar (while H_3Cl^{2+} is not), so that the lone pair electrons must by symmetry occupy regions of space above and below the molecular plane, as in the case of the planar ammonia inversion transition state.[14,24]

The cases of SiH_2^{2-} and CH_2^{2-} (not shown) are more complicated because, while they do indeed show the expected

TABLE 3: Geometry Data for the $HP(CH)_n$ and $HN(CH)_n$ Species from Both Nuclear and ELF Basin Positions[a]

A. Phosphorus

n	∠HPlp	∠CPC′	∠(at)P(at)′	r_{lp}	r_{PH}	N_{lp}
2	126.5	46.7	82.0	1.092	1.427	2.63
3	120.8	74.8	90.2	1.112	1.430	2.27
4	120.1	92.0	93.4	1.120	1.427	2.25
5	120.0	98.7	95.2	1.123	1.430	2.20
PH_3	122.8			1.108	1.424	2.13

B. Nitrogen

n	∠HPlp	∠CNC′	∠(at)N(at)′	r_{lp}	r_{NH}	N_{lp}
2	121.5	60.6	93.2	0.721	1.020	2.59
3	112.6	90.5	103.4	0.732	1.018	2.26
4	109.1	109.2	109.6	0.724	1.014	2.22
5	109.3	112.4	109.0	0.742	1.020	2.17
NH_3	111.2			0.759	1.018	2.15

[a] Angles (degrees) involving the phosphorus or nitrogen hydrogen and its lone pair (∠HPlp−∠HNlp), phosphorus and nitrogen and their neighboring carbon nuclei (∠CPC′, ∠CNC′), and the PC and NC bond basins (∠(at)P(at)′, ∠(at)N(at)′), the P/N lone pair (r_{lp}) and P/NH (r_{PH}) distances (Å), and lone pair basin populations (N_{lp}, numbers of electrons) about phosphorus/nitrogen. Pertinent data for PH_3 and NH_3 are included for comparison.

bean-shaped double lone pair basin, they also exhibits two other basins in the same plane as the lone pair basin but at greater distances from the non-hydrogen nucleus. There is no obvious explanation at this point for this effect. (One of the reviewers correctly points out that the ELF topology for anions such as these is sensitive to basis set, and that if the diffuse and proton polarization functions are omitted (a 6-31G(d) basis), the "normal" situation of just two lone pair basins obtains. It is curious that the presence of a more complete basis (6-31+G(d,p)) would complicate matters. Clearly, there is more to learn about the ELF topology in cases such as these.) A further complication is that while SiH_2^{2-} does ultimately exhibit two lone pair attractors for the major lone pair basins, such is not the case for CH_2^{2-}. This is why angle data can be reported in Table 1 for SiH_2^{2-} but not for CH_2^{2-}. We can calculate R_i^{lp} values for both compounds by referencing the totality of lone pair basins, and the results are unexceptional and fit in well with the other hydrides.

The Effect of Ring Strain: Cyclic Phosphines and Amines

The simple cyclic phosphines and amines ($HP(CH_2)_n$ and $HN(CH_2)_n$ with $n = 2$ to $n = 5$) present an opportunity to study the effect of ring size on the disposition of the phosphorus and nitrogen lone pairs. The NMR shielding properties of the phosphines was studied several years ago[25] because their phenyl-substituted counterparts, $PhP(CH_2)_n$, show an interesting variation in the phosphorus NMR shieldings. The shielding does not vary uniformly with ring size, but rather the smallest ring ($n = 2$) has the highest shielding while the next smallest ($n = 3$) has the lowest shielding. Hartree−Fock calculations in the gauge-including atomic orbital (GIAO) approach on the simpler hydrogen derivatives reproduced this trend in shielding and allow a qualitative understanding of the experimental observations.[25]

Here we study the disposition of the phosphorus and nitrogen lone pairs as a function of ring size (*n*) and determine what, if any, consequences there are as the formal ring bond angles are constrained as the ring is made smaller. The basic data are shown in Table 3 where both geometry and population data are given

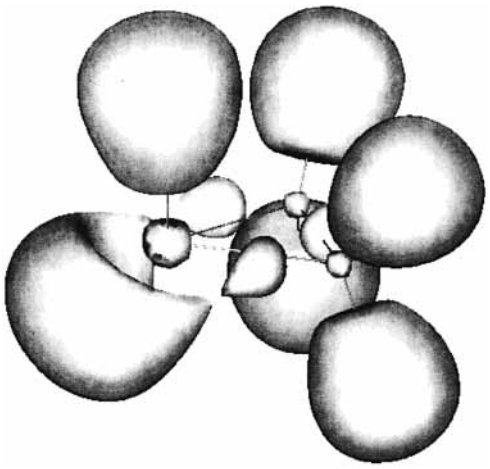

Figure 2. B3LYP/6-31+G(d)//B3LYP/6-31+G(d) ELF isosurfaces for $HP(CH_2)_2$ for $\eta = 0.84$. The phosphorus lone pair basin is in the lower left of the figure.

SCHEME 1

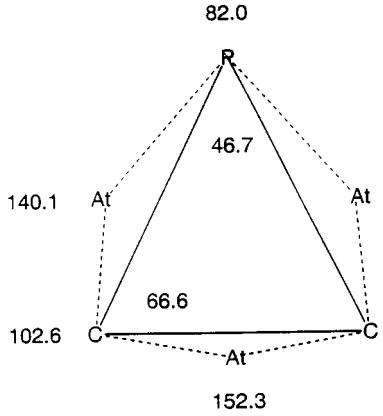

for the phosphorus and nitrogen species. We see that the lone pair distances, r_{lp}, change only slightly for phosphorus compared to PH_3 while for nitrogen a more noticeable change occurs, although still small (5%). In both cases there is a significant increase in the lone pair basin populations upon ring formation and decreasing *n*. While the phosphorus and nitrogen lone pairs character show small but noticeable changes in the $n = 3-5$ cases, for the highly strained $n = 2$ case the HP(N)lp angles show a significant increase.

The strained nature of the rings can be assessed by the angles the heavy atoms make with each other compared to those involving the PC (NC) and CC bond basins. Figure 2 shows the ELF $\eta = 0.84$ isosurface for phosphirane ($n = 2$), and it is clear that both the PC and CC bond basin centers lie outside the triangle formed by the heavy atoms. Table 3 lists the ∠CPC′ and ∠(at)P(at)′angles (where "at" represents a bond basin attractor site) and the schematic above (Scheme 1) illustrates the heavy atom ring and the various angles involved for the $n = 2$ case; the angles inside the triangle are the nuclear geometry angles while those at the vertexes outside correspond to the pertinent angles involving the nuclear centers and the bonding basins. While the CPC′ and CNC′ angles are very small for the $n = 2$ cases, the location of the corresponding bond attractors clearly reveals bent single bonds to be in place. Such bent single bonds have been previously noted.[26-28] The attractor bond angles approach expected values as *n* increases, but note that for the case of the basically unconstrained rings ($n = 5$) the CPC′ and CNC′ bond basin attractor angles are slightly smaller than the corresponding nuclear angles; such behavior has also

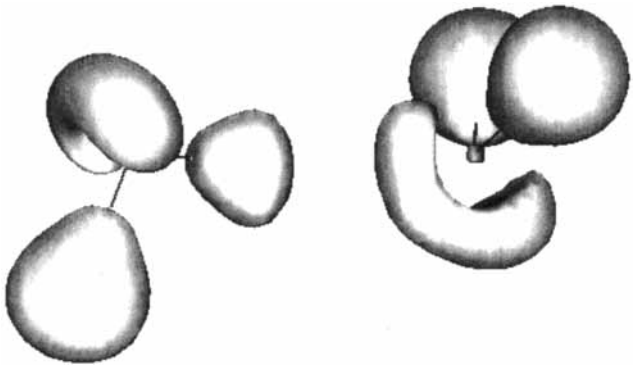

Figure 3. B3LYP/6-31+G(d)//B3LYP/6-31+G(d) ELF isosurfaces for the HOH···OH_2 dimer for $\eta = 0.86$. The water donor is to the left in the figure and the acceptor to the right.

SCHEME 2

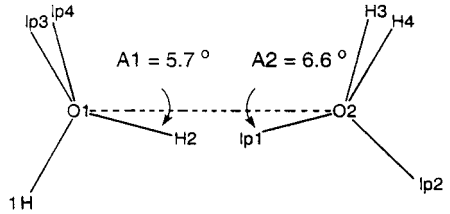

been observed in the AIM topological analysis of 5- and six-membered carbon rings.[4]

Several Cases Involving Hydrogen Bonds

Certainly one of the most important roles of lone pairs is in hydrogen bonding in which the lone pair of the proton acceptor molecule attractively interacts with (usually) an adjacent hydrogen on a proton donor molecule. In previous ELF treatments Noury et al.[12] mention the $(HF)_2$ dimer and Krokidis et al.[29] discuss how bonds change in malonaldehyde during intramolecular proton transfer. Furster and Silvi[19] have the most extensive ELF treatment of hydrogen bonding to date and discuss a variety of situations involving weak (such as the water dimer, HOH···OH_2), intermediate (such as the FH···NH_3 dimer), and strong (such as the FHF^- anion) hydrogen bonds. Krokidis and co-workers[30] have extensively studied the bonding in $(H_2OHOH_2)^+$, a strong hydrogen bonding case.

In the cases involving strong hydrogen bonds the ELF isosurfaces differ significantly in the dimer relative to the isolated monomers and the nature of the lone pairs changes radically. We limit our study here to two cases that maintain the basic character of the lone pairs and investigate how ELF reflects the bonding interaction in the water dimer, a weak hydrogen bond according to Fuster and Silvi,[19] and the dimer involving ammonia and hydrofluoric acid, an intermediate case. For the record we report the binding energies in these two cases to be 4.50 kcal/mol for HOH···OH_2 and 12.60 kcal/mol for FH···NH_3 at the B3LYP/6-311++G(3df,2p)//B3LYP/6-31+G(d) level where both counterpoise[31] and monomer distortion corrections are employed.

A sketch of the water dimer geometry is given in Scheme 2 above while Figure 3 exhibits the ELF $\eta = 0.86$ isosurfaces; for the most part the ELF picture is very much like that of two isolated water molecules, reflective of the weak nature of the interaction. In the dimer molecular geometry changes occur for essentially only the interacting proton and its involved lone pair. These are small for the water dimer, the interacting proton bond distance increasing by 0.009 Å and the interacting lone pair

SCHEME 3

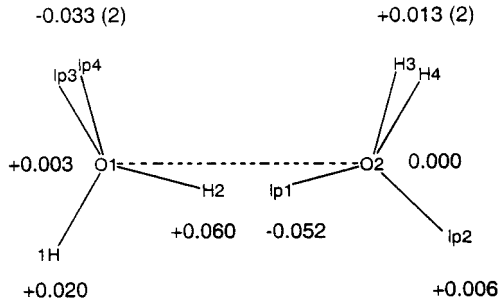

SCHEME 4

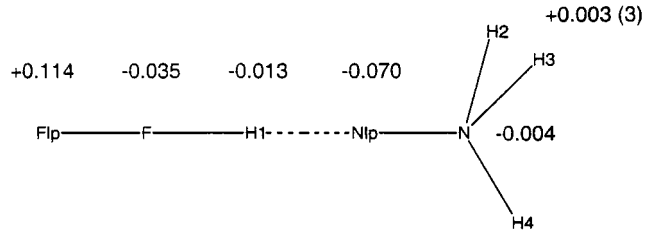

distance (to its parent nucleus) decreasing by 0.005 Å, minor changes at best. The lone pair distances from their parent nucleus do not differ much from that in monomeric water (0.584 Å), being 0.585 Å for lone pairs 3 and 4 and 0.583 Å for lone pairs 1 and 2. Whereas the lone-pair/lone-pair angle is 107.6° in the monomer, the angles in the dimer are 103.5° (lone pairs 3 and 4) and 106.4° (lone pairs 1 and 2). In short, given the limitations of the TopMod code, one cannot discern significant differences in the dispositions of the lone pairs in the monomer and in the dimer. Scheme 2 shows that at our B3LYP/6-31+G(d) optimized geometry the O2−O1−H2 angle is 5.7° while the O1−O2-lp1 angle is 6.6°; if this lone pair were to point directly at H2, this latter angle should be 2.9°. The difference between the "ideal" and observed angles is of borderline significance. It is noteworthy, however, that both the donated proton and the accepting lone pair depart significantly from the O1−O2 line; this is well-known for the donor proton, but now we have shown it to also be true for the lone pair attractor interacting with the donor proton.

The *changes* in basin populations of the water dimer relative to monomeric water are shown above in Scheme 3 where the number 2 in parentheses indicates the population changes of *each* of two lone pairs. It is clear, as one might have expected, that the major change is a transfer of about 0.05−0.06 of an electron from the interacting lone pair (lp1) to the proton (H2) with which it interacts. This is larger than the overall shift of charge from the basins of the accepting water molecule to those of the donor water, a figure of 0.018. This agrees with the corresponding shift of charge found from an AIM analysis of 0.028. Studying trends of the basin populations as one changes the equilibrium O−O distance, one sees smooth and monatomic trends supporting the idea that, while the changes are small, they are realistic.

The case for FH···NH_3 is similar to that of the water dimer but does differ in significant ways. The strength of the bond in this dimer is revealed by significant changes in the geometry. The fluorine proton bond distance increases by 0.041 Å and the nitrogen lone pair distance decreases by a large 0.112 Å, from 0.759 to 0.647 Å. Scheme 4 above shows the population changes of the dimer relative to the isolated monomers; each of the three nitrogen lone pairs exhibits a change of +0.003. The acceptor lone pair loses charge but so also does the

SCHEME 5

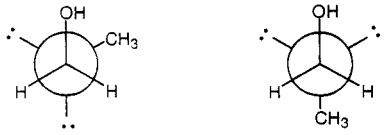

SCHEME 6

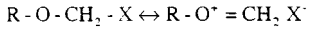

SCHEME 7

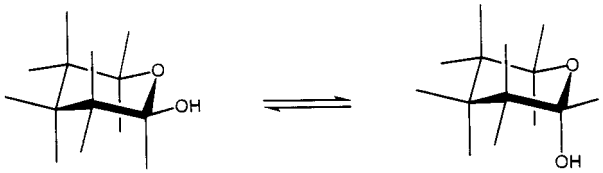

hydrogen bonding fluorine proton; in this example the charge transferred is 0.066 to the HF moiety and accumulates mainly on the fluorine lone pair. This likely reflects the strong electronegativity of fluorine. Again, as with the water dimer, while the changes are small, studies of the basin populations as a function of the monomer−monomer separation shows a smooth and monatomic trend.

The Anomeric Effect

The anomeric effect in organic stereochemistry, considered by many to be the most important polar factor in the conformational analysis of saturated heterocyclic systems, is discussed in great depth in the books by Eliel, Wilen, and Mander[32] and Juaristi and Cuevas.[33] It is reflected in the fact that the equilibrium between β-D-glucose and α-D-glucose is much less favoring of the β form over the α form than would be expected on steric repulsion grounds alone. Indeed, in the case of the methyl glucosides where a methoxy group replaces the OH neighboring the ring oxygen, it is actually the α anomer that is favored. The effect was first given its name by Limeaux and Chu.[34]

The generalized anomeric effect[35,36] implies that in a molecule such as methoxymethanol, $HOCH_2OCH_3$, the gauche form is preferred over the anti isomer (Scheme 5). Romers et al.[37] point out that there are two ways of rationalizing this effect.

First, in the anti form both lone pairs of the central oxygen can interact with the hydroxy oxygen as opposed to only one such interaction in the gauche form. Since these interactions are expected to be repulsive, this favors the gauche form. These authors go on to point out that a likely more viable model is one in which in the $ROCH_2X$ fragment a double-bond-no-bond resonance occurs (Scheme 6), stabilizing the gauche form. That is, in molecular orbital terms, in the gauche form one of the oxygen lone pair orbitals overlaps favorably with the σ^* antibonding orbital of the neighboring carbon. Both the lone pair repulsion argument and the σ^* resonance stabilization of the OC bond will lead to a detectable shortening of the OC bond compared to situations in which the anomeric effect cannot occur.

In the present case we looked at the simpler ring equilibrium of 2-hydoxy-tetrahydropyran (Scheme 7) and in particular detail at the gauche and anti forms of the relevant fragment involving the $HOCH_2OCH_3$ molecule.

For both the cyclic and acyclic examples the axial forms are lower in energy at the B3LYP/6-311++G(3df,2p)//B3LYP/6-31+G(d) level, by 2.34 kcal/mol for the acyclic system and 1.10 kcal/mol for the cyclic one. The corresponding changes in the enthalpy (2.11 and 0.80 kcal/mol, respectively) and the Gibbs free energies (1.84 and 0.59 kcal/mol) also show the axial species to be lower in energy than the equatorial forms. Consistent with what has been observed for other anomeric species, the oxygen−methoxy−carbon distances are reduced in the axial species relative to the equatorial forms: 1.404 Å versus 1.415 Å in the acyclic compound and 1.418 Å versus 1.426 Å for the cyclic compound. On the other hand, the bond between the methoxy carbon and the methoxy oxygen is longer for the axial species, 1.414 Å versus 1.394 Å for the acyclic compound and 1.421 versus 1.400 for the cyclic compound. Both these results are consistent with the double-bond/no-bond resonance form presented earlier.

TABLE 4: ELF Parameters for the Axial (ax) and Equatorial (eq) Methoxymethanol Compounds[a]

	axial	equatorial
N_{lp}	2.447[b]	2.476
	2.418	2.423
N_{OC}	1.387	1.337
r_{lp}	0.580[b]	0.577
	0.581	0.579
∠lp−lp	111.8	120.8
∠lp−bb	109.5 ± 0.5	107.0 ± 0.4
∠bb−bb	107.0	107.5

[a] N_{lp} and N_{OC} are the basin populations for the central oxygen lone pairs and the adjoining OC bond basin (electrons), r_{lp} (Å) represents the oxygen lone pair distances from the oxygen atom core, and the angles are measured about the oxygen core for the lone pairs with each other (∠lp−lp), the mean lone pair/bond basin angle (∠lp−bb), and the bond basins with each other (∠bb−bb), all in degrees [b] This lone pair is that in which a favorable interaction with the carbon σ^* orbital could occur.

We can contrast these results for the dioxy compounds to those where the ether oxygen is replaced by a methylene group (cyclohexanol and propanol). In these cases it is the equatorial or anti forms which are stabler, 0.40 kcal/mol for propanol and 0.77 kcal/mol for cyclohexanol. Furthermore, the bond length changes in the mono-oxy cases are minimal, always less than 0.007 Å.

ELF calculations were done only for the smaller methoxymethanol compounds. For the most part only very small changes are noted. There are, however, several data that reveal some interesting behavior, as shown in Table 4. The lone pair radii are virtually identical in the axial and equatorial species and essentially equal to the radii for other oxygen lone pairs. That lone pair favorably located to interact with the neighboring carbon σ^* orbital (noted in the table) has a slightly reduced electron population that shows up as an increase in the oxygen−carbon bond basin. This is consistent with the double-bond/no-bond resonance model. Although the population differences are small on an absolute scale for the TopMod code, we believe the *changes* to be significant. Recall that in the water dimer, another example of a weak interaction, charge transfer of the order of 0.05−0.06 electron is likely the signature of the dimer bound by 4.50 kcal/mol. Here in methoxymethanol the transferred charge is smaller, 0.03−0.05 electrons, but then so is the energy difference between the axial and equatorial forms, 2.34 kcal/mol

The other notable feature is the fact that while the various basin angles about the central oxygen are more or less the same for the axial compound, the lp−lp angle is greatly increased in the equatorial case compared to the axial case by 112 to 121 degrees, a not insignificant increase. It is tempting to ascribe

this to the expected lone-pair/exterior-oxygen repulsions in the anti form that are not present in the gauche form.

Changes in ELF isosurfaces and the electron populations contained therein are subtle and we do not yet have a full understanding of their complexities. And certainly while our results do not prove the double-bond/no-bond σ^* orbital interaction model, they are strongly supportive.

Summary

The electron localization function is a very useful way of characterizing not only chemical bonds and core electrons but also those electrons not strongly involved with bonding, the lone pairs. The nuclear charge basically determines the character of an attached lone pair although the molecular charge can affect the volume over which the lone pair is found. While lone pair geometries and basin populations differ only in small ways in different isomers or when molecules are weakly interacting, the *changes* are significant and provide us further information in characterizing the interactions.

Acknowledgment. I am indebted to the North Carolina Supercomputing Center for providing CPU time on the Cray T-916 and SGI Origin 2000 platforms that allowed these calculations to be carried out, to Dr. L. J. Bartolotti for help with the TopMod and AVS visualization programs, and to Professor S. W. Baldwin for helpful discussions. The journal referees provided a number of helpful comments.

References and Notes

(1) Gillespie, R. J.; Nyholm, R. S. *Q. Rev.* **1957**, *11*, 334.
(2) Gillespie, R. J. *Molecular Geometry*; Van Nostrand Reinhold: London, 1972.
(3) Gillespie, R. J.; Hargittai, I *VSEPR Model of Molecular Geometry*; Allyn and Bacon, Boston, 1991. Gillespie, R. J.; Robinson, E. A. *Angew. Chem.* **1996**, *108*, 539; *Angew Chem. Int. Ed. Engl.* **1996**, *35*, 495.
(4) Bader, R. F. *Atoms in Molecules: A Quantum Theory*; Oxford University Press: Oxford, U.K., 1994.
(5) Becke, A. D.; Edgecombe, K. E. *J. Chem. Phys.* **1990**, *92*, 5397.
(6) Savin, A.; Becke, A. D.; Flad, J.; Nesper, R.; Preuss, H.; von Schnering, H. G. *Angew Chem. Int. Ed. Engl.* **1991**, *30*, 409.
(7) Silvi, B.; Savin, A. *Nature* **1994**, *371*, 683.
(8) Savin, A.; Silvi, B.; Colonna, F. *Can. J. Chem.* **1996**, *74*, 1088.
(9) Kohout, M.; Savin, A. *Int. J. Quantum Chem.* **1996**, *60*, 875.
(10) Savin, A.; Nesper, R.; Wengert, S.; Fässler, T. *Angew Chem., Int. Ed. Engl.* **1997**, *36*, 1809.
(11) Marx, D.; Savin, A. *Angew. Chem., Int. Ed. Engl.* **1997**, *36*, 2077.
(12) Noury, S.; Colonna, F.; Savin, A.; Silvi, B. *J. Mol. Struct.* **1998**, *450*, 59.
(13) Kouhout, M.; Savin, A. *J. Comput. Chem.* **1997**, *18*, 1431.
(14) Krokidis, X.; Noury, S.; Silvi, B. *J. Phys. Chem. A* **1997**, *101*, 7277.
(15) Fourre, I.; Silvi, B.; Chaquin, P.; Sevin, A. *J. Comput. Chem.* **1999**, *20*, 897.
(16) Fuster, F.; Silvi, B. *Chem. Phys.* **2000**, *252*, 279.
(17) Fuster, F.; Sevin, A.; Silvi, B. *J. Phys. Chem. A* **2000**, *104*, 852.
(18) Silvi, B.; Gatti, C. *J. Phys. Chem. A* **2000**. *104*, 947.
(19) Furster, F.; Silvi, B. *Theor. Chem. Acc.* **2000**, *104*, 13.
(20) Noury, S.; Krokidis, X.; Fuster, F.; Silvi, B. *Comput. Chem.* **1999**, *23*, 597.
(21) Becke, A. D. *J. Chem. Phys.* **1993**, *98*, 5648.
(22) Lee, C.; Yang, W.; Paar, R. G. *Phys. Rev.* **1988**, *B 37*, 785.
(23) Frisch, M. J.; Trucks, G. W.; Schlegel, H. B.; Scuseria, G. E.; Robb, M. A.; Cheeseman, J. R.; Zakrzewski, V. G.; Montgomery, J. A., Jr.; Stratmann, R. E.; Burant, J. C.; Dapprich, S.; Millam, J. M.; Daniels, A. D.; Kudin, K. N.; Strain, M. C.; Farkas, O.; Tomasi, J.; Barone, V.; Cossi, M.; Cammi, R.; Mennucci, B.; Pomelli, C.; Adamo, C.; Clifford, S.; Ochterski, J.; Petersson, G. A.; Ayala, P. Y.; Cui, Q.; Morokuma, K.; Malick, D. K.; Rabuck, A. D.; Raghavachari, K.; Foresman, J. B.; Cioslowski, J.; Ortiz, J. V.; Baboul, A. G.; Stefanov, B. B.; Liu, G.; Liashenko, A.; Piskorz, P.; Komaromi, I.; Gomperts, R.; Martin, R. L.; Fox, D. J.; Keith, T.; Al-Laham, M. A.; Peng, C. Y.; Nanayakkara, A.; Gonzalez, C.; Challacombe, M.; Gill, P. M. W.; Johnson, B.; Chen, W.; Wong, M. W.; Andres, J. L.; Gonzalez, C.; Head-Gordon, M.; Replogle, E. S.; Pople, J. A. *Gaussian 98*, Revision 7; Gaussian, Inc.: Pittsburgh, PA, 1998.
(24) Chesnut, D. B. *J. Phys. Chem. A* **2000**, *104*, 7635.
(25) Chesnut, D. B.; Quin, L. D.; Wild, S. B. *Heteroatom Chem.* **1997**, *8*, 451.
(26) Savin, A.; Flad, H.-J.; Flad, J.; Preuss, H.; von Schnering, H. J. *Angew. Chem., Int. Ed. Engl.* **1992**, *31*, 185.
(27) Chesnut, D. B. *Heteroatom Chem.* **2000**, *11*, 73.
(28) Choukroun, R.; Donnadieu, B.; Zhao, J.-S.; Cassoux, P.; Lepetit, C.; Silvi, B. *Organometallics* **2000**, *19*, 1901.
(29) Krokidis, X.; Goncalves, V.; Savin, A.; Silvi, B. *J. Phys. Chem.* **1998**, *102*, 5065.
(30) Krokidis, X.; Vuilleumier, R.; Borgis, D.; Silvi, B. *Mol. Phys.* **1999**, *96*, 265.
(31) S. F. Boys; S. F.; F. Bernardi, F. *Mol. Phys.* **1970**, *19*, 553.
(32) Eliel, E. L.; Wilen, S. H.; Mander, L. N. *Sterochemistry of Organic Compounds*; John Wiley and Sons: New York, 1994.
(33) Juaristi, E.; Cuevas, G. *The Anomeric Effect*; CRC Press: Boca Raton, FL, 1995.
(34) Lemieux, R. U.; Chu, N. J. Abstract Papers American Chemical Society 133rd Meeting, p 31N, 1958.
(35) Lemieux, R. U. *Pure Appl. Chem.* **1971**, *25*, 527.
(36) Eliel, E. L. *Angew. Chem., Int. Ed. Engl.* **1972**, *11*, 739.
(37) Romers, C.; Altona, C.; Buys, A. R.; Havinga, E. *Top. Stereochem.* **1969**, *4*, 39.